RESEARCH PAPER

Influence of plastic fines content on the liquefaction susceptibility of sands: cyclic loading

Meisam Goudarzy[1] · Debdeep Sarkar[1] 🄳 · Torsten Wichtmann[1]

Abstract

The paper presents an experimental study on the effect of plastic fines content on the undrained behavior and liquefaction susceptibility of sand-fines mixtures under cyclic loading. The results of undrained cyclic triaxial tests conducted on mixtures of Hostun sand with varying amounts (0–20%) and types (kaolin and calcigel bentonite) of plastic fines are presented. The specimens were prepared with different initial densities using the moist tamping method, consolidated at the same isotropic effective stress of 100 kPa and subjected to different deviatoric stress amplitudes. From the experimental observations, it was found that sand-clay mixtures with 10% or 20% clay content showed a lower cyclic liquefaction resistance than pure sand. Furthermore, the reduction in the cyclic stress ratio resulting in liquefaction after twenty cycles was found larger for sand-kaolin mixtures than for the sand-calcigel ones. Possible explanations are provided.

Keywords Cyclic undrained triaxial tests · Liquefaction resistance · Plastic fines content · Sand-fines mixtures

1 Introduction

For regions prone to dynamic or cyclic motions (i.e., earthquakes or other natural and man-made sources), the evaluation of the risk of soil liquefaction represents an important part of a safe design of geotechnical structures. Natural soils usually contain a certain fraction of silty or clayey fines, which may have a detrimental effect on the liquefaction resistance. While the influence of non-plastic fines on the liquefaction resistance under cyclic loading has been extensively investigated [2, 5, 8, 11, 16, 19, 20, 24, 29], the effect of plastic fines has been less often studied. Furthermore, the effect of fines plasticity is still discussed controversially. A literature review regarding the influence of plastic fines on the behavior of sand-fines mixtures under monotonic and cyclic loading has been already published by Goudarzy et al. [13]. The most important studies referring to the liquefaction resistance under cyclic loading are repeated hereafter.

Some early investigations on the liquefaction resistance of granular soils with fines of various plasticity were performed by Ishihara and Koseki [17] and Ishihara [18]. They stated that the liquefaction resistance correlates better with plasticity index than with fines content and that the fines content has an influence only if its plasticity index is greater than 10. In contrast, Koester [21] found fines plasticity to have a lower influence than fines content. Park and Kim [28] tested sand mixed with 10% fines having varying plasticity in the range of 8–377%. For loose samples prepared by moist tamping, the plasticity of the fines did not play a significant role, while for denser specimens, a reduction of up to 40% of the liquefaction resistance was encountered with increasing plasticity. Opposite tendencies with increasing fines plasticity were observed in some other earlier studies [10, 14] and [1]. Marto et al. [25] used sand with white kaolin and green bentonite as fines, and arrived at the conclusion that liquefaction resistance of the sand-fines mixtures increased as the value of plasticity index increased. Papadopoulou and Tika [27] tested clean

✉ Debdeep Sarkar
  debdeep.sarkar@rub.de

  Meisam Goudarzy
  meisam.goudarzyakhore@rub.de

  Torsten Wichtmann
  torsten.wichtmann@rub.de

[1] Chair of Soil Mechanics, Foundation Engineering and Environmental Geotechnics, Ruhr-Universität Bochum, Bochum, Germany

round sand mixed with either non-plastic silt or speswhite kaolin (plasticity index of 35%) using samples prepared by moist tamping. They noted that at a given void ratio and fines content, the degree of contractiveness increased till a threshold plasticity index, after which specimens with higher plasticity index exhibited higher liquefaction resistance. In another recent study utilizing cyclic simple shear tests by Eseller-Bayat et al. [9], clean sand showed a higher liquefaction resistance than any sand-non-plastic silt/plastic clay mixtures tested under a given relative density. Furthermore, the influence of plasticity increased with higher fines content and relative density. The addition of 10% of plastic fines leads to a lower liquefaction resistance compared to the same amount of non-plastic fines, which was attributed to water retention characteristics of clay contributing to forming a lubricating coating around sand grains.

Considering the few available and partly contradictory experimental studies in the literature, the objective of the present work was a thorough investigation of the influence of two different types of plastic fines content differing in plasticity on the cyclic behavior and the liquefaction resistance of Hostun sand. In the series of undrained cyclic triaxial tests, beside the plasticity, the amount of fines (0, 10 and 20%), the initial relative density of the samples and the deviatoric stress amplitude were varied. A comprehensive discussion of the experimental observations is provided.

2 Experimental program

2.1 Tested materials

Three different base materials were used from which four different sand-clay mixtures were prepared: Hostun sand as the host sand and Amberg kaolin and calcigel bentonite as plastic fines. The two fine clays were chosen based on their popularity in the literature as well as the fact that extensive previous test results may be found for these materials (e.g., [31, 34, 36] and the references therein).

Hostun sand is a poorly graded medium quartz sand with grain sizes between 0.1 and 1 mm (mean grain size $d_{50} = 0.35$ mm and uniformity coefficient $C_u = d_{60}/d_{10} = 1.58$). The limit void ratios e_{max} and e_{min} were determined as 1.04 and 0.67, respectively [12]. Based on a grain shape analysis, the roundness and circle-ratio sphericity values (see [35] are 0.40 and 0.75, respectively. Amberg kaolin with a plasticity index $I_P = 19.1\%$ and calcigel bentonite ($I_P = 58.8\%$) was used to study the influence of varying clay content and plasticity. Amberg kaolin is a natural kaolinite-based clay, while calcigel bentonite is a montmorillonite clay with calcium as the

exchangeable cation [3]. Further details about the physical properties of the materials are listed in Table 1. Both clays are highly plastic (as determined by the Casagrande apparatus) since both have a liquid limit $w_L > 50\%$. Figure 1 shows the grain size distribution curves of the three tested materials. Mixtures of Hostun sand with 10% and 20% plastic fines were used in the present study. The maximum and minimum void ratios for the dry sand-kaolin mixtures determined following the experimental procedures of the DIN 18126 [7] recommendations were 1.184 and 0.576 (for 10% fine content) and 1.423 and 0.436 (for 20% fines), respectively. For the sand-calcigel mixtures, the values of e_{max} and e_{min} were 1.060 and 0.581 for 10% fines, and 1.045 and 0.552 for 20% fines (see [13]).

2.2 Test device

The tests were performed on an electro-mechanically driven cyclic triaxial device manufactured by Wille Geotechnik GmbH, Germany, shown in Fig. 2. The loading was applied at a constant strain rate of 0.3 mm/min till the input stress amplitude was reached followed by reversal of loading. Samples measuring 10 cm in diameter and 20 cm in height were used. Smeared end plates with a porous stone covering the whole cross-sectional area of the sample were applied. Axial load was measured at a load cell located below the sample base plate. Axial deformation was measured through displacement sensors (LVDT) attached at the top of the loading bar, whereas the volume changes were controlled using a volume pressure controller (VPC). Cell and back pressure were measured with pressure transducers. During the cyclic loading phase data were continuously recorded every second using the PC and a data acquisition system.

Table 1 Physical characteristics of the adopted fine materials

		Amberg kaolin	Calcigel bentonite
Main mineral		Kaolinite	Montmorillonite
Liquid limit w_L	%	56.1	103.1
Plastic limit w_P	%	38.0	43.3
Plasticity Index I_P	%	19.1	58.8
Specific gravity	–	2.64	2.79
Cation exchange capacity (CEC)[a]	meq/100 g	5	64
Specific surface area (SSA)[b]	m²/g	32	525

[a]Cu-Triethylenetetramine [26]
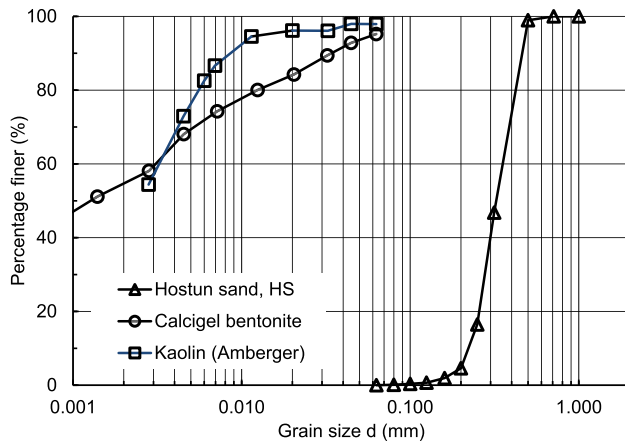
[b]Ethylene glycol monoethyl ether (EGME) [6]

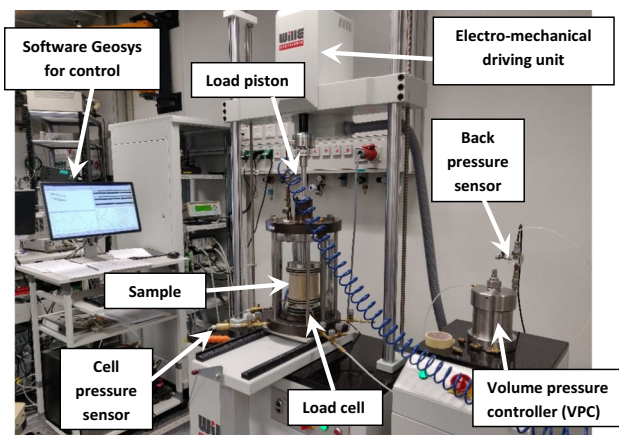Fig. 1 Grain size distribution of the adopted materials

Fig. 2 Schematic representation of the cyclic triaxial device used for the experiments

2.3 Sample preparation

The samples were prepared using the moist tamping (MT) method. The main advantage of MT over air pluviation (AP) is that particle segregation during sample preparation is minimized, ensuring a homogenous gradation throughout the sample. Furthermore, obtaining both loose and dense specimens of mixtures with predefined target densities is comparatively more straightforward through MT.

The dry sand and clay powder were initially mixed by hand in corresponding proportions of 10 and 20% by weight, followed by water addition until a homogenous mixture was obtained. To ensure homogenous water distribution throughout the sample, the samples were kept in a sealed container for 12 h. The initial water contents of the triaxial samples, which were similar to those used in the monotonic tests on the same mixtures reported by Goudarzy et al. [13], are given in Table 2.

A mold lined with the latex membrane of thickness 0.7 mm was mounted on the pedestal of the triaxial cell.

The prepared material was then placed in the mold in eight layers of 2.5 cm thickness each. After weighting the material for each layer, it was filled into the mold, distributed evenly over the cross-sectional area, and compacted to the desired density using a plastic tamper. The layer thickness was checked by measuring the distance from the upper edge of the mold to the layer surface for all the layers.

The triaxial cell was subsequently filled with water, and the cell pressure was increased steadily while reducing the vacuum temporarily used for sample stabilization during the preparation process. At a cell pressure of 50 kPa, CO_2 was circulated through the sample for 1 h, followed by saturation with de-aired de-mineralized water until no visible air bubbles emerged from the outlet of the drainage lines. The sample was then subjected to higher magnitudes of cell and back pressure (240 and 200 kPa, respectively) to dissolve the majority of the remaining air to ensure the best possible saturation. The sample was consolidated at the desired effective stress p_0' of 100 kPa, which was achieved by increasing the cell pressure to 300 kPa while keeping the back pressure constant at 200 kPa. During consolidation, both volume and axial deformation changes were measured continuously. The void ratios and relative densities $I_D = (e_{max} - e)/(e_{max} - e_{min})$ of all samples after the consolidation phase are provided in Table 2, with the latter calculated based on the e_{min} and e_{max} values introduced in Sect. 2.1.

After consolidation the drainage was closed and undrained cyclic loading was started. The behavior of the samples observed in the tests is discussed in detail in the next section. Some samples failured by flow liquefaction, characterized by the sudden development of large deformations within a single cycle. In those tests a state with zero effective stress is usually not reached. The onset of flow liquefaction was defined as the failure criterion for those tests. In other tests the samples showed cyclic mobility, that means a gradual increase in the axial strain amplitude with each further cycle after initial liquefaction, and the typical butterfly-shaped effective stress path. In those tests the initial liquefaction, defined as reaching a state of zero effective stress for the first time, was chosen as failure criterion. The tests that failed via flow liquefaction and cyclic mobility are marked as FL and CM, respectively, in Table 2.

3 Experimental results

3.1 Liquefaction resistance of clean Hostun sand

Clean Hostun sand was tested with two different relative densities ($I_D = 0.27 - 0.30$ and $0.55 - 0.59$) and varying

Table 2 Schedule of the tests performed using Hostun sand as the host material and kaolin and calcigel as the plastic fines

Test name	Sand content (%)	Clay	Clay content (%)	Initial water content (%)	I_D (–)	e (–)	p_0' (kPa)	B-value (–)	q_{ampl} (kPa)	Failure mode
TZ-HS-1	100	–	0	9.2	0.59	0.826	100	0.92	40	CM
TZ-HS-2	100	–	0	9.7	0.57	0.834	100	0.93	50	CM
TZ-HS-3	100	–	0	10.1	0.55	0.843	100	0.90	60	CM
TZ-HS-4	100	–	0	9.0	0.30	0.943	100	0.85	20	FL
TZ-HS-5	100	–	0	9.0	0.27	0.953	100	0.92	40	FL
TZ-10Kao-1	90	Kaolin	10	8.0	0.60	0.818	100	0.95	15	FL
TZ-10Kao-2	90	Kaolin	10	8.0	0.62	0.809	100	0.95	20	FL
TZ-10Kao-3	90	Kaolin	10	7.9	0.60	0.818	100	0.95	25	FL
TZ-20Kao-1	80	Kaolin	20	14.0	0.77	0.660	100	0.95	25	FL
TZ-20Kao-2	80	Kaolin	20	14.5	0.81	0.623	100	0.96	30	FL
TZ-10Cal-1	90	Calcigel	10	13.3	0.61	0.766	100	0.92	25	CM
TZ-10Cal-2	90	Calcigel	10	14.6	0.60	0.769	100	0.93	30	CM
TZ-10Cal-3	90	Calcigel	10	14.0	0.58	0.781	100	0.94	40	CM
TZ-20Cal-1	80	Calcigel	20	18.5	0.63	0.733	100	0.95	25	CM
TZ-20Cal-2	80	Calcigel	20	18.5	0.65	0.723	100	0.96	30	CM

stress amplitudes q_{ampl} (refer to Table 2) to obtain the curves of cyclic stress ratio CSR = $q_{ampl}/(2p_0')$ versus the number of cycles to either flow liquefaction (reaching a minimum of 8% axial strain) or initial liquefaction (cyclic mobility characterized by butterfly shaped loops). Figure 3 shows the deviatoric stress against the mean effective stress (Fig. 3a, b) or the axial strain (Fig. 3c, d), respectively, for two tests on medium dense samples with different deviatoric stress amplitudes q_{ampl} = 40 kPa (TZ-HS-1, Fig. 3a, c or 60 kPa (TZ-HS-3, Fig. 3b,d). For both tests, a typical cyclic mobility behavior is observed, with the amplitude of axial strain increasing with each further cycle after initial liquefaction. It is clear that increasing the amplitude of deviatoric stress results in a lower number of cycles to failure and hence, faster liquefaction. The sample loaded with q_{ampl} = 40 kPa requires 214 cycles till initial liquefaction, while 13 cycles are needed in case of q_{ampl} = 60 kPa. The curves of CSR versus the number of cycles to initial liquefaction are shown in Fig. 3e for the two different relative densities, showing the well-known density-dependence of the liquefaction resistance. The data are also compared with test results from the literature [22] on the same sand under similar boundary conditions. The

slight differences between both test series, particularly for the denser samples, may result from a slightly different batch of Hostun sand used by Krim et al. [22], with a larger mean grain size of 0.47 mm.

3.2 Influence of the clay content

(a) **Kaolin contents of 10% and 20%**

The q–p' and the q–ε_1 paths for mixtures of Hostun sand with either 10% or 20% kaolin subjected to a stress amplitude of 20 kPa corresponding to a CSR of 0.10 are shown in Fig. 4. The 20% kaolin sample shows a significantly faster reduction in the mean effective stress with the application of cyclic loading than the 10% kaolin sample, even though the initial relative density is larger (I_D = 0.81 versus 0.62). Both samples show a failure by flow liquefaction, characterized by a sudden increase in axial deformation accompanied by a strong reduction in mean effective stress p'. The 20% kaolin sample fails after 11 cycles, while the 10% kaolin sample can carry 26 cycles. The development of pore water pressure u against time for both specimens is compared in Fig. 4e, confirming the
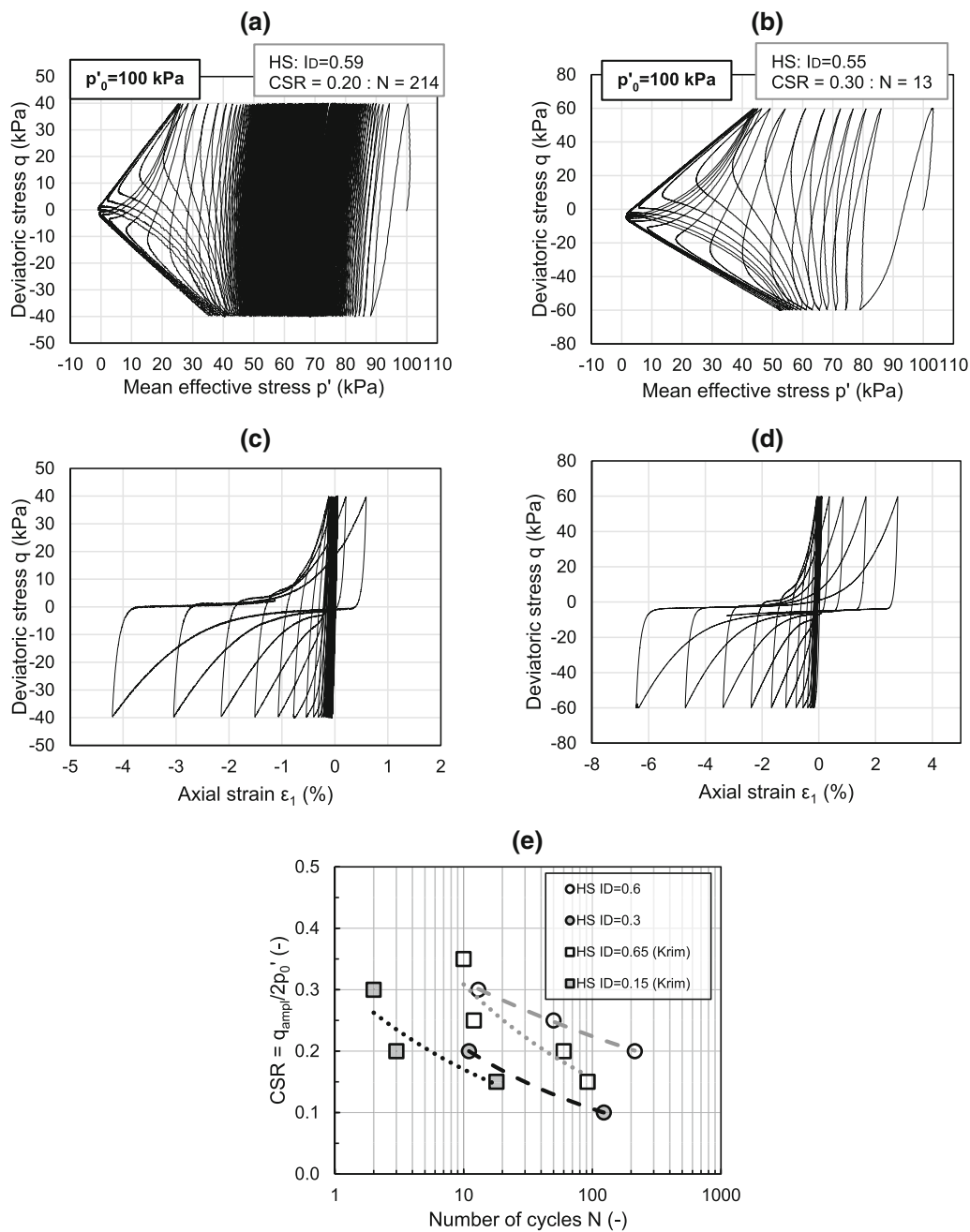
Fig. 3 Response of Hostun sand under two CSR values (CSR = 0.2 and 0.3): **a** and **b** effective stress paths, **c** and **d** deviatoric stress–axial strain relationship, **e** cyclic stress ratio versus the number of cycles to liquefaction in comparison with the studies of Krim et al. [22]

faster increase in u for the 20% kaolin specimen. Owing to the termination of the test at large axial strain (8% in extension), u does not reach the same magnitude as the isotropic total stress applied (300 kPa). This can be also seen from the effective stress paths, where the point of failure is associated with a mean effective stress $p_0' > 0$.

(b) **Calcigel contents of 10% and 20%**

For the sand-calcigel mixtures with either 10% or 20% fines content the results of tests with a deviatoric stress

amplitude of q_{ampl} = 25 kPa, corresponding to CSR = 0.125, are provided in Fig. 5. In contrast to the sand-kaolin mixtures, the samples containing calcigel as the fines show a cyclic mobility type failure (Fig. 5a–d). Compared to clean Hostun sand (Fig. 3), however, a lower number of cycles could be applied in the cyclic mobility phase before reaching large strains (8% was chosen as the failure criterion here). Comparing both tests a stronger decrease in the mean effective stress p' per loading cycle for the higher calcigel content is evident from Fig. 5. The
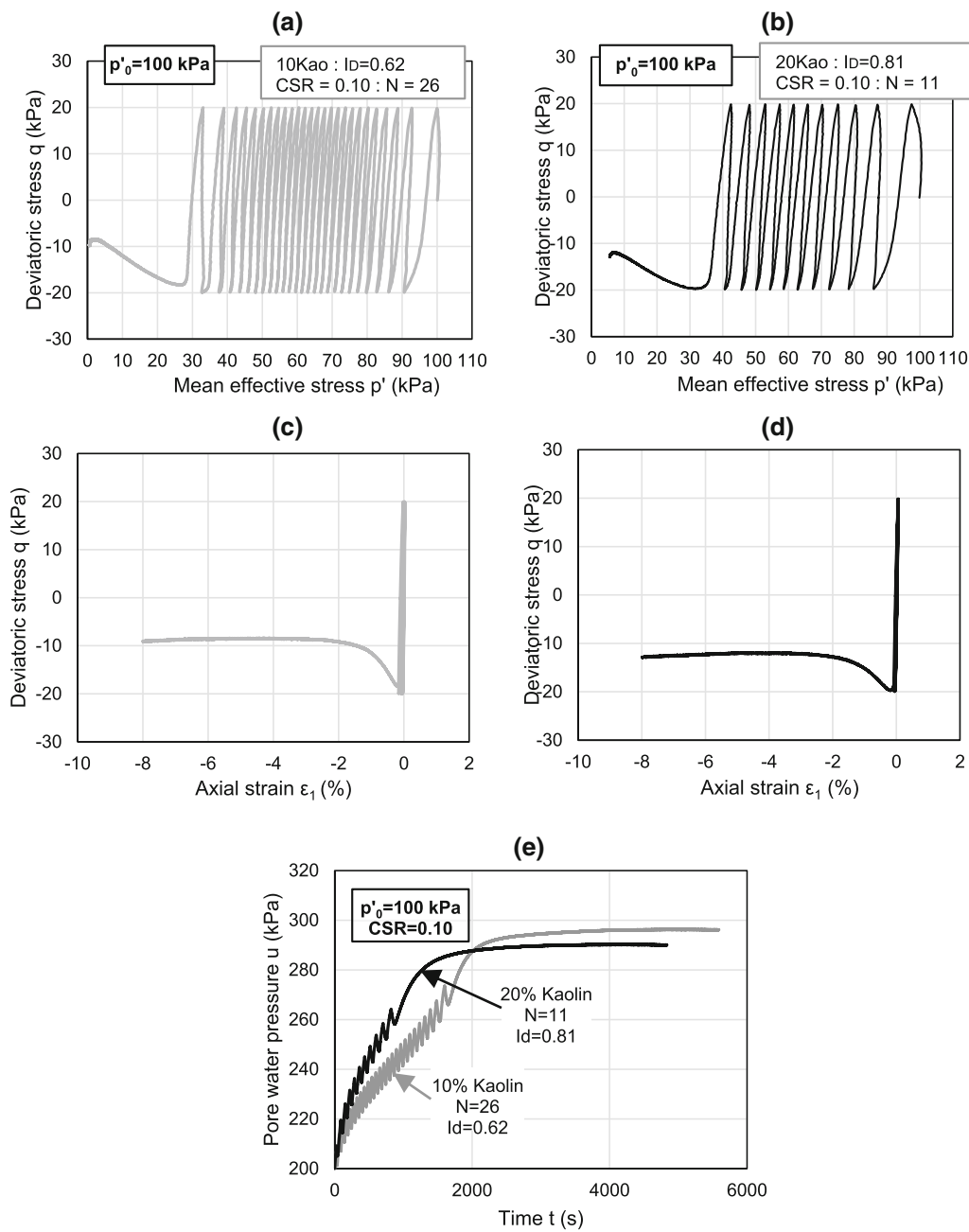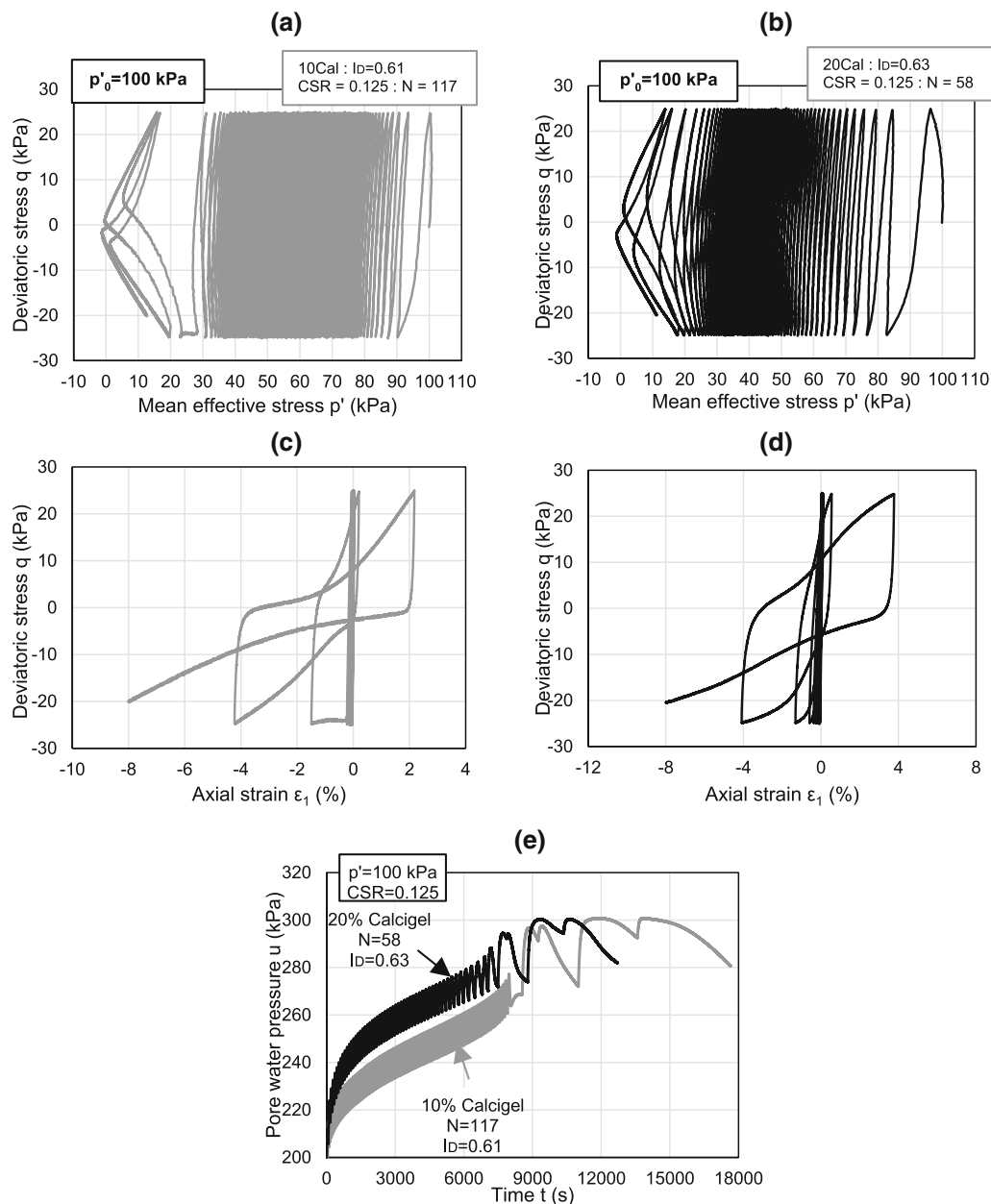
Fig. 4 Response of Hostun sand-kaolin mixtures with two fines contents (10% and 20%): **a** and **b** effective stress paths, **c** and **d** deviatoric stress–axial strain relationship, **e** development of the pore water pressure with time

10% calcigel sample takes 117 cycles for initial liquefaction, while the same is achieved after 58 cycles for the 20% calcigel sample, at comparable relative densities. The faster pore water pressure accumulation of the 20% calcigel specimen is also visible in Fig. 5e, where the pore water pressure variation is plotted against time.

3.3 Influence of the clay type

To study the influence of clay type in more detail, a comparison of the effective stress paths and pore water pressure versus time relationships is done in Fig. 6, for two specimens having a similar relative density, clay content and subjected to an identical CSR (= 0.125). The sample

Fig. 5 Response of Hostun sand-calcigel mixtures with two fines contents (10% and 20%): **a** and **b** effective stress paths, **c** and **d** deviatoric stress–axial strain relationship, **e** development of the pore water pressure with time

with 10% kaolin content requires only 6 cycles to achieve flow liquefaction (Fig. 6a). In contrast, the sample containing 10% calcigel can sustain a significantly larger number of cycles until initial liquefaction occurs (117 cycles), and two cycles can be applied in the cyclic mobility phase until an axial strain of 8% is reached in extension (Fig. 6b). The reduction in the effective stresses in the kaolin sample is significantly faster, implying a much faster rise of the pore water pressure than in the sample containing calcigel (Fig. 6c).

3.4 Influence of relative density

The influence of the relative density of the specimens was studied by comparing samples of clean Hostun sand and those containing 10% calcigel content at two different relative densities I_D, which are approximately 30 and 60%. The results are plotted in the CSR-N space in Fig. 7. The well-known increase in the liquefaction resistance with increasing density is evident for both the clean Hostun sand and the sand-calcigel mixtures (although there is an anomaly for the sand-fines mixture at CSR = 0.2, where
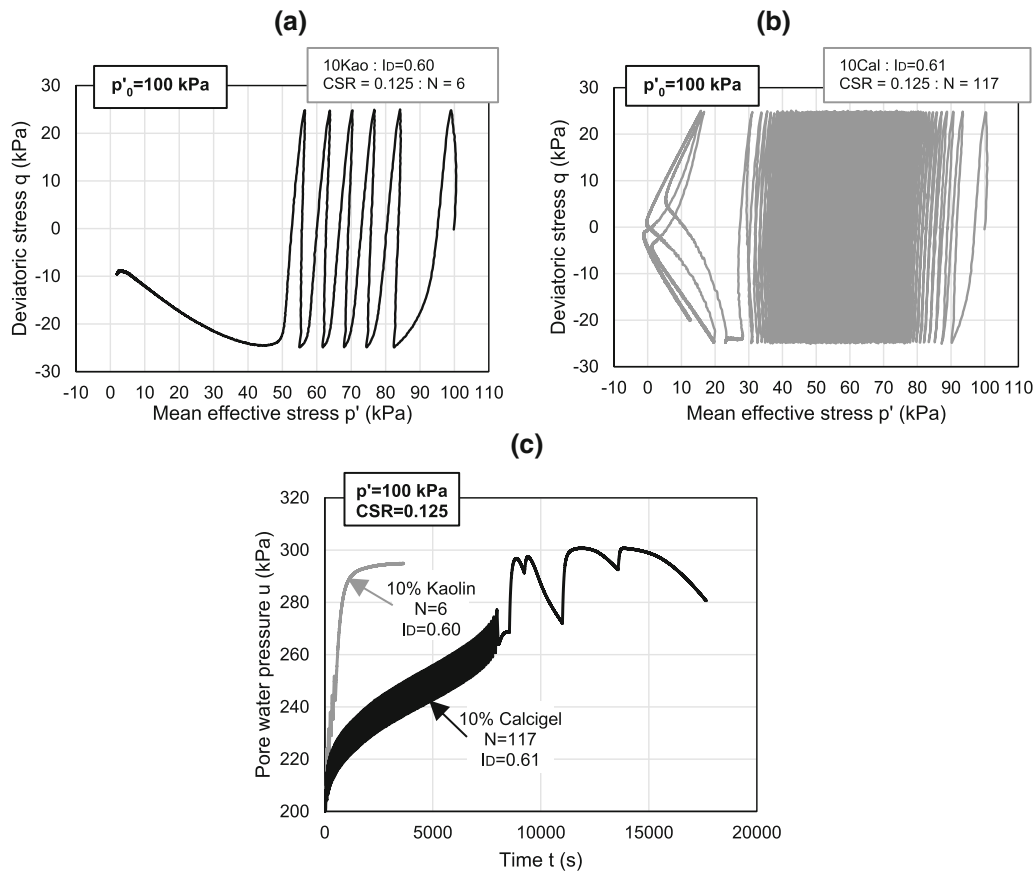
Fig. 6 Effective stress paths of Hostun sand-kaolin/calcigel mixtures at 10% fines content: **a** kaolin, **b** calcigel, **c** development of the pore water pressure with time for the above two cases
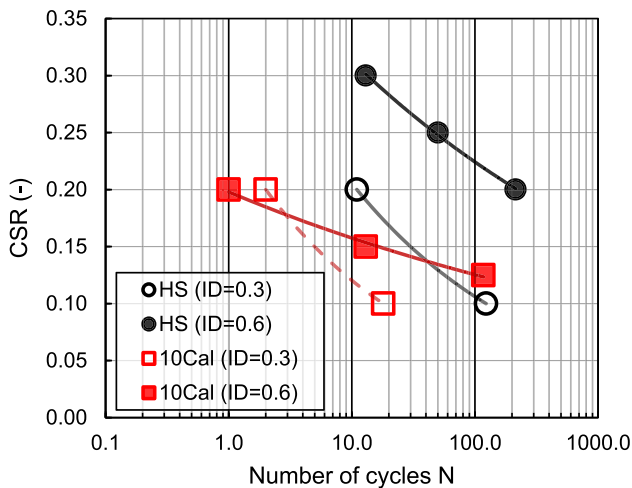

Fig. 7 Cyclic stress ratio CSR versus number of cycles to liquefaction N for the clean Hostun sand and the mixture of sand with 10% calcigel under two relative densities (approx. 0.3 and 0.6)

the looser sample shows a later liquefaction). Furthermore, for a given relative density, the clean sand requires a larger number of cycles to liquefy when subjected to the same CSR. For example, in the case of the specimens having a relative density of about 30% and considering a CSR of 0.20, the clean sand requires 10 cycles, while the mixture of sand and 10% calcigel liquefied at the end of the second cycle. The same can also be evidenced for the medium dense specimens (ID about 60%) where at CSR = 0.20 the clean sand requires 217 cycles, while the sand-kaolin mixture is liquefied in only one cycle.

4 Cyclic resistance ratio (CRR_{20})

The CSR-N plots for the two different clay contents 10% and 20% are shown in Fig. 8. In these diagrams it is evident that an increase in the clay content irrespective of the clay type results in a downward shift of the trend line. However, the drop in the liquefaction resistance from the clean host sand to the mixtures with 10% kaolin or calcigel is much more pronounced than the drop from 10 to 20% fines content. The cyclic stress ratio required to liquefy the specimens at the 20th cycle is defined as the cyclic resistance ratio (CRR_{20}), which is utilized for the further analysis.
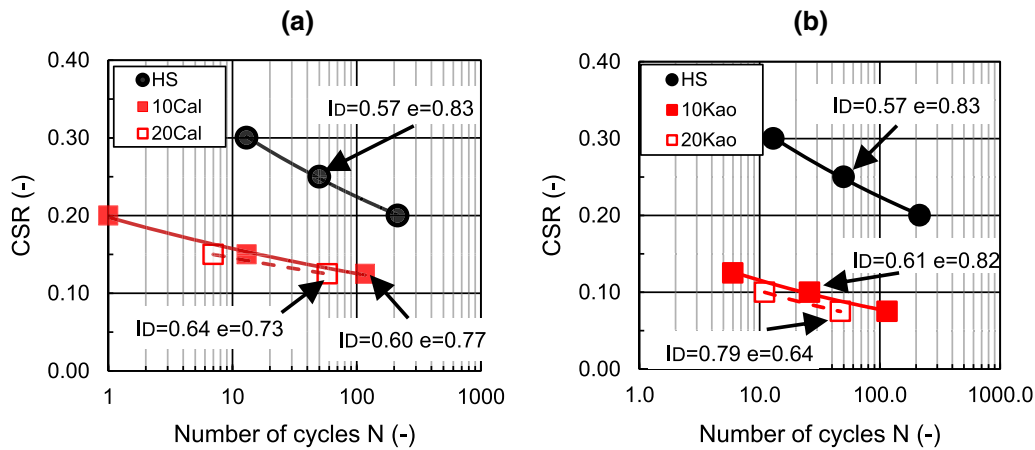
Fig. 8 Cyclic stress ratio CSR versus number of cycles to liquefaction N for the various mixtures: **a** Hostun + calcigel, **b** Hostun + kaolin
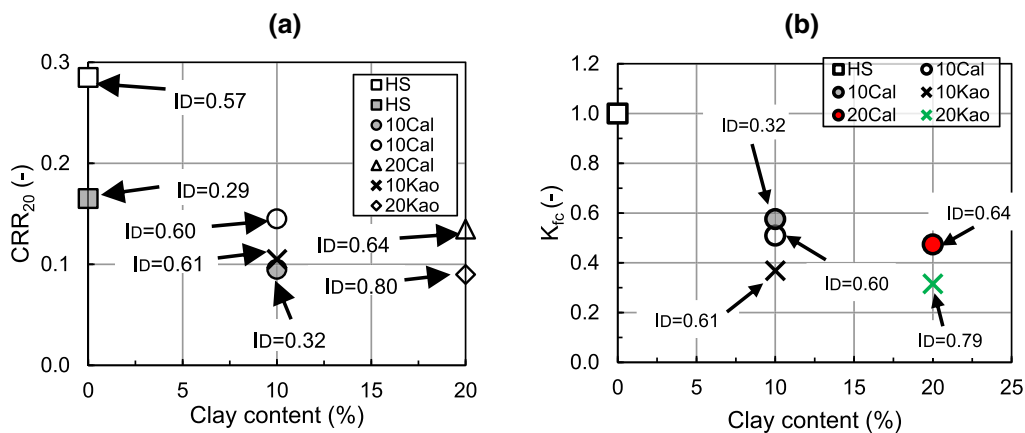

Fig. 9 Variation of the **a** CRR_{20}, and **b** K_{fc} against the clay content

The variation of the CRR_{20} against the clay content for different relative densities is shown in Fig. 9a. It is clear that for both clay types with increasing clay content, CRR_{20} decreases. Also, dense specimens of the sand with the same clay type have a higher CRR_{20} compared to looser ones. For the mixtures with 10% clay content, the variation of $K_{fc} = CRR_{fc \neq 0}/CRR_{fc=0}$ ($CRR_{fc=0} = CRR$ of clean host sand, $CRR_{fc \neq 0} = $ corresponding value of the sand-fines mixture for certain relative densities against 10% and 20% clay contents and is shown in Fig. 9b. Interestingly, for the sand and 10% calcigel mixture, the K_{fc} for the looser sample ($I_D = 32\%$) is slightly larger than that for the denser one ($I_D = 60\%$). Also, for the kaolin specimen, the K_{fc} value is larger than for the calcigel specimen, which implies that the decrease of CRR_{20} is more pronounced for the kaolin mixtures than for the calcigel ones. This is further supplemented by the results obtained from the medium dense mixtures (I_D around 60%) of the two sand-fine mixtures-the value of K_{fc} for the 20% calcigel mixture ($I_D = 0.64$) remains higher than that of the

20% kaolin mixture (tested at higher $I_D = 0.79$), thereby providing additional proof that the sand-kaolin mixtures show a faster decrease in CRR_{20} than the sand-calcigel mixture considering fines content up to 20%.

4.1 Variation of CRR_{20} with void ratio and relative density

The variation of the CRR_{20} against the global void ratio is shown in Fig. 10a. Although the void ratios of the different mixtures at similar relative density vary due to the different e_{min} and e_{max} values, for a constant void ratio a decrease in the liquefaction resistance with increasing fines content can be concluded from Fig. 10a. This decrease is more pronounced for the kaolin than for the calcigel fines content, and stronger between 0 and 10% than for the range between 10 and 20% fines content. Similar conclusions can be drawn for a constant relative density, when looking at the CRR_{20} versus relative density I_D data in Fig. 10b.
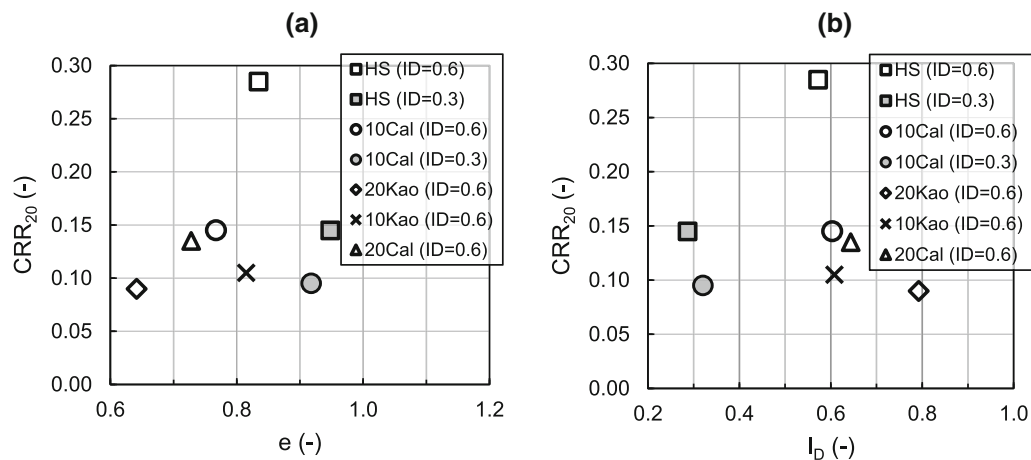
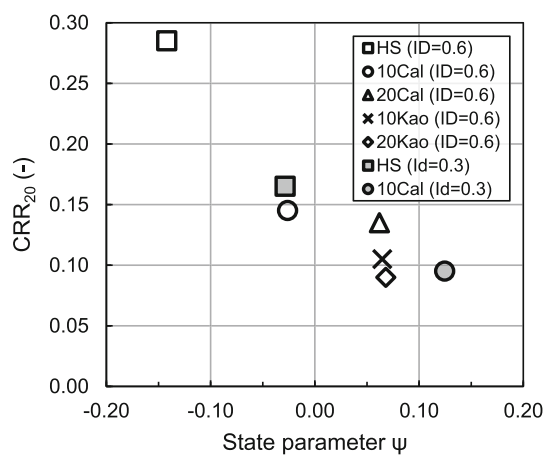**Fig. 10** Variation of CRR_{20} against **a** global void ratio e, **b** relative density I_D

Fig. 11 Variation of the CRR_{20} against the global state parameter ψ

4.2 Variation of the CRR_{20} against state parameter

Furthermore, Fig. 11 shows the variation of CRR_{20} against the state parameter $\psi = e - e_{cs}$. The steady-state/critical state lines (SSL/CSL) determined from undrained monotonic triaxial tests and already presented in Goudarzy et al. [13] were used to calculate the void ratio e_{cs} at the steady-state and the state parameter under a certain pressure. For the clean Hostun sand and each mixture, a separate SSL was set into approach for the determination of e_{cs}. A nonlinear equation was used for the SSL of clean Hostun sand, while for the mixtures, a logarithmic relationship was adopted [13]. Evidently, both negative and positive ψ were considered in the present analysis. With increasing state parameter the material response becomes more contractive and the liquefaction resistance decreases. From Fig. 11 one can conclude that CRR_{20} correlates fairly well with the state parameter, almost independently of the type and amount of plastic fines.

5 Discussion of results

The available studies in the literature have pointed out controversial observations regarding the influence of the plasticity of the fines on the liquefaction resistance. On the one hand, based on traditional geotechnical engineering knowledge it could be assumed that increasing plasticity of the fines content in granular soils leads to an increase in the liquefaction resistance [9], and certain studies have backed up this statement [1, 10, 14]. Papadopoulos and Tika stated a threshold value above which liquefaction resistance was found to increase for highly plastic fines, although the plasticity values tested were rather small ($I_P = 6$ and 22). However, some studies (e.g., [9, 28] have shown the opposite tendencies. Park and Kim [28] reasoned that in case of silty fines dilatancy enhanced the liquefaction resistance, while for clayey fines a reduction in friction between sand-fine interfaces resulted in a loss of strength. Eseller-Bayat et al. [9] postulated that plastic clays form a coating on the surface of the sand particles acting as a lubricant, which might increase volumetric contractiveness and therefore liquefaction susceptibility, although acknowledging the requirement of further evidence to back up their claims.

However, the results in the present study, showing a higher liquefaction resistance for fines of higher plasticity, go against the observations of a couple of above-mentioned studies. There can be a couple of reasons associated with it. In the case of kaolinite, the bonding between successive layers is achieved through both van der Waals forces and hydrogen bonds. However, in calcigel bentonite, the bonding between successive layers results from van der Waals forces and cations that balance charge deficiencies in the structure which can be easily broken when water seeps into these pores. Furthermore, soils containing plastic fines are more susceptible to liquefaction due to the

forming of an open micro-fabric, in which clay aggregations gathered at the sand particle contacts serve as low-strength connectors [14]. The difference in the responses between the two types of clay can be attributed to the differences in the bonding between the sand particles caused by the fines. Kaolinite behaves as very fine silt soils consisting of quartz grains with low specific surface area,hence the coating is more irregular and contains a larger number of large particles [15]. Therefore, such mixtures show a more contractive behavior and a faster accumulation of excess pore water pressure under undrained conditions [23, 30, 33, 37–39], implying a lower number of cycles to liquefaction. However, for clays with higher plasticity like calcigel, the coating is smooth and regular around the sand particles [14, 32], leading to a stronger bonding than in case of kaolin.

Another possible explanation may be based on the presence of free pore water: Owing to strong bonding, kaolinite lamellae do not disperse into smaller units upon water addition. In contrast, the weak bonding in the calcigel layers permits further separation into very small flakes [15]. Since adsorbed water is more viscous than free pore water, it helps to hold the calcigel-coated sand grains together, which is lacking in the saturated sand-kaolin mixture [4, 13]. Since there is larger free pore water in the sand-kaolin mixtures, the soil fabric is more collapsible,as a consequence, excess pore water pressures can thus develop more easily, which is reflected in the lower number of cycles to liquefaction.

A similar trend can be found in comparing the monotonic test results documented in Goudarzy et al. [13] with the cyclic ones presented herein. In the monotonic tests, increasing the plasticity of fines resulted in less contractive response, higher instability stress ratios and higher strengths at a given fines content and under otherwise similar boundary conditions (relative density and confining pressure). In the present study, the observations run along similar lines, albeit with respect to the CRR values.

6 Conclusions

A series of undrained cyclic triaxial tests were conducted on clean Hostun sand and Hostun sand mixed with two different amounts of two different clays (10% and 20%), kaolin and calcigel bentonite to assess their liquefaction resistance. Mixtures of the sand with both types of clay show a more pronounced contractive behavior and lower undrained cyclic strength at comparable relative densities than the clean Hostun sand. Furthermore, for the same clay content, the specimens containing kaolin liquefy faster than those mixed with calcigel. This means that the liquefaction resistance increases with increasing plasticity of the fines.

While the samples of sand-kaolin mixtures failed due to flow liquefaction, a cyclic mobility type failure was observed for the sand-bentonite mixtures. The cyclic resistance ratio CRR_{20} for a liquefaction in 20 cycles was found to correlate well with the state parameter ψ. Possible explanations of the differences between the two types of clays based on interparticle bonding or amount of free and absorbed pore water were provided.

References

1. Ajmera B, Brandon T, Tiwari B (2017) Influence of index properties on shape of cyclic strength curve for clay-silt mixtures. Soil Dyn Earthq Eng 102:46–55

2. Akhila M, Rangaswamy K, Sankar N (2019) Undrained response and liquefaction resistance of sand-silt mixtures. Geotech Geol Eng 37(4):2729–2745

3. Baille W (2014) Hydro-mechanical behaviour of clays—significance of mineralogy. PhD thesis, Ruhr-Universität Bochum, Germany

4. Beroya MAA, Aydin A, Katzenbach R (2009) Insight into the effects of clay mineralogy on the cyclic behavior of silt–clay mixtures. Eng Geol 106:154–162

5. Bouckovalas G, Andrianopoulos K, Papadimitriou A (2003) A critical state interpretation for the cyclic liquefaction resistance of silty sands. Soil Dyn Earthq Eng 23(2):115–125

6. Cerato A, Lutenegger A (2002) Determination of surface area of fine-grained soils by the ethylene glycol monoethyl ether (EGME) method. Geotech Test J 25(3):315–321

7. DIN18126 (1996) Baugrund, Untersuchung von Bodenproben—Bestimmung der Dichte nichtbindiger Böden bei lockerster und dichtester Lagerung. Germany

8. Enomoto T (2019) Liquefaction and post-liquefaction properties of sand-silt mixtures and undisturbed silty sands. Soils Found 59(6):2311–2323

9. Eseller-Bayat EE, Monkul MM, Akin Ö, Yenigun S (2019) The coupled influence of relative density, CSR, plasticity and content of fines on cyclic liquefaction resistance of sands. J Earthq Eng 23(6):909–929

10. Ghahremani M, Ghalandarzadeh A, Ghahremani K (2007) Laboratory investigation of the effect of plastic fines on cyclic resistance of sand-clay mixtures. In: 4th International conference on earthquake geotechnical engineering

11. Gobbi S, Reiffsteck P, Lenti L, d'Avila MPS, Semblat J (2022) Liquefaction triggering in silty sands: effects of non-plastic fines and mixture-packing conditions. Acta Geotech 17:391–410

12. Goudarzy M, Rahman MM, König D, Schanz T (2016) Influence of non-plastic fines content on maximum shear modulus of granular materials. Soils Found 56(6):973–983

13. Goudarzy M, Sarkar D, Lieske W, Wichtmann T (2021) Influence of plastic fines content on the liquefaction susceptibility of sands: monotonic loading. Acta Geotech. https://doi.org/10.1007/s11440-021-01283-w

14. Gratchev IB, Sassa K, Osipov VL, Sokolov VN (2006) The liquefaction of clayey soils under cyclic loading. Eng Geol 86(2006):70–84

15. Grim RE (1962) Applied clay mineralogy. McGraw-Hill, New York, p 422

16. Hyodo T, Wu Y, Hyodo M (2022) Influence of fines on the monotonic and cyclic shear behaviour of volcanic soil "Shirasu." Eng Geol 301:106591

17. Ishihara K, Koseki J (1989) Discussion on the cyclic shear strength of fines containing sands, earthquake geotechnical engineering. In: Proceedings of the XII international conference on soil mechanics, pp101–106

18. Ishihara K (1993) Liquefaction and flow failure during earthquakes. Geotechnique 43:351–415

19. Karim ME, Alam J (2016) Undrained monotonic and cyclic response of sand–silt mixtures. Int J Geotech Eng 10(3):223–235

20. Kim U, Zhuang L, Kim D, Lee J (2016) Evaluation of cyclic shear strength of mixtures with sand and different types of fines. Mar Georesour Geotechnol 35(4):447–455

21. Koester JP (1994) The influence of fines type and content on cyclic strength, Ground failures under seismic conditions. Geotechnical Special Publication No: 44. ASCE, pp 17–33

22. Krim A, Arab A, Bouferra R, Sadek M, Shahrour I (2016) Characteristics of cyclic shear behavior of sandy soils: a laboratory study. Arab J Sci Eng 41:3995–4005

23. Lade PV, Yamamuro JA (1997) Effects of nonplastic fines on static liquefaction of sands. Can Geotech J 34:918–928

24. Li X, Liu J, Nan J (2022) Prediction of dynamic pore water pressure for calcareous sand mixed with fine-grained soil under cyclic loading. Soil Dyn Earthq Eng 157:107276

25. Marto A, Tan CS, Makhtar AM, Wen US, Yen LM (2015) Effect of plasticity on liquefaction susceptibility of sand-fines mixtures. Appl Mech Mater 773–774:1407–1411

26. Meier LP, Kahr G (1999) Determination of the cation exchange capacity (CEC) of clay minerals using the complexes of copper(II) ion with triethylenetetramine and tetraethylenepentamine. Clays Clay Miner 47:386–388

27. Papadopoulou AI, Tika TM (2016) The effect of fines plasticity on monotonic undrained shear strength and liquefaction resistance of sands. Soil Dyn Earthq Eng 88:191–206

28. Park SS, Kim YS (2013) Liquefaction resistance of sands containing plastic fines with different plasticity. J Geotech Geoenviron Eng 139(5):825–830

29. Polito CP (1999) The effect of non-plastic and plastic fines on the liquefaction of sandy soils. Ph.d., thesis, Virginia Polytechnic Institute and State University

30. Porcino DD, Diano V, Triantafyllidis T, Wichtmann T (2020) Predicting undrained static response of sand with non-plastic fines in terms of equivalent granular state parameter. Acta Geotech 15:867–882. https://doi.org/10.1007/s11440-019-00770-5

31. Proia R, Croce P, Modoni G (2016) Experimental investigation of compacted sand-bentonite mixtures. In: VI Italian conference of researchers in geotechnical engineering-geotechnical engineering in multidisciplinary research: from microscale to Regional Scale, CNRIG2016, 158, pp 51–56

32. Pusch R, Yong RN (2006) Microstructure of smectite clays and engineering performance. Taylor & Francis, London

33. Rahman MM, Lo SR, Baki MAL (2011) Equivalent granular state parameter and undrained behavior of sand–fines mixtures. Acta Geotech 6:183–194. https://doi.org/10.1007/s11440-011-0145-4

34. Rawat A (2019) Coupled hydro-mechanical behavior of a compacted bentonite-sand mixture: experimental and numerical investigations. Ph.d. thesis, Ruhr-Universität Bochum

35. Sarkar D, König D, Goudarzy M (2019) The influence of particle characteristics on the index void ratios ingranular materials. Particuology 46:1–13. https://doi.org/10.1016/j.partic.2018.09.010

36. Wichtmann T, Triantafyllidis T (2018) Monotonic and cyclic tests on Kaolin—a data base for the development, calibration and verification of constitutive models for cohesive soils with focus to cyclic loading. Acta Geotech 13(5):1103–1128

37. Xenaki VC, Athanasopoulos GA (2003) Liquefaction resistance of sand–silt mixtures: an experimental investigation of the effect of fines. Soil Dyn Earthq Eng 23(3):1–12

38. Yang J, Wei LM (2012) Collapse of loose sand with the addition of fines: the role of particle shape. Geotechnique 62(12):1111–1125

39. Yang J, Liu X (2016) Shear wave velocity and stiffness of sand: the role of non-plastic fines. Geotechnique 66(6):500–514